Geochemistry Geophysics Geosystems G3
AN ELECTRONIC JOURNAL OF THE EARTH SCIENCES
Published by AGU and the Geochemical Society

Technical Brief
Volume 9, Number 8
9 August 2008
Q08Y02, doi:10.1029/2008GC001976
ISSN: 1525-2027

AMSSpin: A LabVIEW program for measuring the anisotropy of magnetic susceptibility with the Kappabridge KLY-4S

Jeffrey S. Gee and Lisa Tauxe
Geosciences Research Division, Scripps Institution of Oceanography, University of California, San Diego, La Jolla, California 92093-0220, USA (jsgee@ucsd.edu)

Cathy Constable
Institute of Geophysics and Planetary Physics, Scripps Institution of Oceanography, University of California, San Diego, La Jolla, California 92093-0225, USA

[1] Anisotropy of magnetic susceptibility (AMS) data are widely used as a petrofabric tool because the technique is rapid and nondestructive and because static measurement systems are capable of determining small degrees of anisotropy. The Kappabridge KLY-4S provides high resolution as a result of the large number of measurements acquired while rotating the sample about three orthogonal axes. Here we describe a graphical-based program called AMSSpin for acquiring AMS data with this instrument as well as a modified specimen holder that should further enhance the utility of this instrument. We also outline a method for analysis of the data (that differs in several ways from that of the software supplied with the instrument) and demonstrate that the measurement errors are suitable for using linear perturbation analysis to statistically characterize the results. Differences in the susceptibility tensors determined by our new program and the SUFAR program supplied with the instrument are small, typically less than or comparable to deviations between multiple measurements of the same specimen.

Components: 6177 words, 13 figures.

Keywords: magnetic fabric; AMS; susceptibility tensor; Kappabridge.

Index Terms: 1518 Geomagnetism and Paleomagnetism: Magnetic fabrics and anisotropy; 1594 Geomagnetism and Paleomagnetism: Instruments and techniques.

Received 4 February 2008; **Revised** 17 June 2008; **Accepted** 27 June 2008; **Published** 9 August 2008.

Gee, J. S., L. Tauxe, and C. Constable (2008), AMSSpin: A LabVIEW program for measuring the anisotropy of magnetic susceptibility with the Kappabridge KLY-4S, *Geochem. Geophys. Geosyst.*, *9*, Q08Y02, doi:10.1029/2008GC001976.

Theme: Advances in Instrumentation for Paleomagnetism and Rock Magnetism
Guest Editor: V. Salters

1. Introduction

[2] The magnetic fabric of rocks, as quantified by anisotropy of magnetic susceptibility (AMS) measurements, has been used as a petrofabric proxy in a wide variety of geological applications (see reviews by *Rochette et al.* [1992] and *Tarling and Hrouda* [1993]). Magnetic susceptibility data

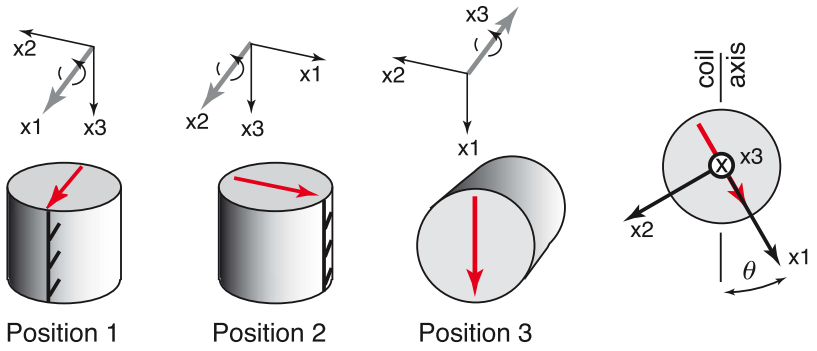

Figure 1. Specimen orientations for the three spins used with the Kappabridge KLY-4S. The heavy gray arrow (oriented toward the user for spins one and two and away from the user for spin three) shows the axis of rotation. The orientation of the specimen coordinate system in space is specified by the azimuth and plunge of either the arrow along the core length (+x3 axis, black) or the +x1 axis (red arrow on core top). Right-hand figure shows orientation of applied field (coil axis) relative to specimen coordinates in position 3.

provide a rapid, nondestructive means of characterizing the volumetric preferred alignment of magnetic phases with sufficient precision to recognize very slight degrees of anisotropy (<1%) that are difficult to quantify with other techniques. The recently developed Kappabridge KLY-4S and earlier KLY-3S [*Jelinek and Pokorny*, 1997; *Pokorny et al.*, 2004] allow even higher precision determination of the magnetic susceptibility tensor by acquiring substantially more susceptibility data as the sample is rotated in three orthogonal planes.

[3] We describe here a new program called AMSSpin for acquiring AMS data from the Kappabridge KLY-4S. AMSSpin is designed to provide a user friendly environment for perhaps the most common type of measurement (AMS) made with the Kappabridge; other useful features of the instrument (e.g., temperature-dependent measurements) are not incorporated into our program. The principal advantages of the program are the real time display of susceptibility data acquired during a spin (we use the term spin to indicate data from multiple revolutions) and the display of best fit 2-D and 3-D models to the data as well as the resulting residuals. These data allow the user to evaluate instrument drift and the signal-to-noise ratio and to identify some errors resulting from misorientation or poor centering of the specimen. Eigenvectors for the current specimen can be plotted together with previously measured data (in a variety of coordinate systems) to allow evaluation of within site consistency. The processing of data differs from that of the SUFAR program supplied with the instrument, which is based on the Jelinek theory [*Jelinek*, 1995] of measuring the AMS of a slowly spinning specimen, both in terms of analyzing data from one spin as well as in the determination of the six independent elements of the best fit tensor. Differences in the susceptibility tensors determined by our new program and the SUFAR program supplied with the instrument are small, typically less than or comparable to deviations between multiple measurements of the same specimen. Finally, we have designed a cubic sample holder for core samples that allows more reproducible positioning of the sample in three orthogonal orientations (Appendix A).

2. Theory

[4] Magnetic susceptibility is a second-order tensor relating the induced magnetization of a sample to the applied magnetic field. Relative to the coordinate system (x_1, x_2, x_3) of the sample (Figure 1), the susceptibility tensor may be expressed as

$$\mathbf{K} = \begin{bmatrix} k_{11} & k_{12} & k_{13} \\ k_{21} & k_{22} & k_{23} \\ k_{31} & k_{32} & k_{33} \end{bmatrix}$$

where $k_{ij} = k_{ji}$ for i $\neq$ j. The six independent elements of the susceptibility tensor may be designated by a vector **s**, with elements k_{11}, k_{22}, k_{33}, $k_{12} = k_{21}$, $k_{23} = k_{32}$, $k_{13} = k_{31}$.

[5] Magnetic susceptibility instruments measure the directional susceptibility (D), i.e., the susceptibility in the direction parallel to the coil axis. In a static measurement system, the directional susceptibility is measured in six or more orientations (e.g., a series of 15 measurements in three orthogonal planes is typically used for the Kappabridge KLY-2 system [*Jelinek*, 1977, 1978]). The orientation of the applied field (relative to the specimen

coordinate system) for each of these n measurements is described by an $n \times 6$ matrix termed the design matrix (**A**). The n directional susceptibility values (**D**) are related to the design matrix and **s** by

$$\mathbf{D} = \mathbf{A}\mathbf{s} \tag{1}$$

and the best fit values ($\bar{\mathbf{s}}$) of **s** in a least squares sense may be calculated from

$$\bar{\mathbf{s}} = \left(\mathbf{A}^T\mathbf{A}\right)^{-1}\mathbf{A}^T\mathbf{D} \tag{2}$$

The best fit values may, in turn, be used to estimate residuals (δ_i) for each of the measurements.

$$\delta_i = D_i - A_{ij}\bar{s}_j \tag{3}$$

In a slowly spinning specimen measurement system such as the Kappabridge KLY-4S, directional susceptibility can be measured as the specimen is rotated in each of three orthogonal planes [see *Jelinek*, 1995], clockwise about the $+x_1$ axis, clockwise about the $+x_2$ axis and counterclockwise about the $+x_3$ axis (Figure 1). The directional susceptibility signal as the specimen is rotated about the $+x_1$ axis (D^{x1}) is given by

$$D^{x1} = \begin{bmatrix} 0 & \sin(\theta) & \cos(\theta) \end{bmatrix} \begin{bmatrix} k_{11} & k_{12} & k_{13} \\ k_{12} & k_{22} & k_{23} \\ k_{13} & k_{23} & k_{33} \end{bmatrix} \cdot \begin{bmatrix} 0 \\ \sin(\theta) \\ \cos(\theta) \end{bmatrix}$$

where θ is the angle of the applied field relative to the sample coordinate system. Directional susceptibility values are recorded for 64 positions during each revolution, and the value for the ith angular measurement about the $+x_1$ axis is given by

$$D_i^{x1} = k_{22}\sin^2(\theta_i) + 2k_{23}\cos(\theta_i)\sin(\theta_i) + k_{33}\cos^2(\theta_i)$$

We will refer to this as the 2-D model that describes the directional susceptibility during rotation about one of the sample coordinate axes. Combining three such models (one from rotation about each of the sample coordinate axes) allows calculation of a 3-D model. In a similar fashion, the values for the ith angular measurement about the $+x_2$ and $+x_3$ axes are given by

$$D_i^{x2} = k_{11}\sin^2(\theta_i) - 2k_{13}\cos(\theta_i)\sin(\theta_i) + k_{33}\cos^2(\theta_i)$$
$$D_i^{x3} = k_{22}\sin^2(\theta_i) + 2k_{12}\cos(\theta_i)\sin(\theta_i) + k_{11}\cos^2(\theta_i)$$

By analogy with (1) above for the static measurement system, the 192 directional susceptibility values acquired during these three spins are related to the six independent elements of the susceptibility tensor by a 192×6 design matrix (**A**):

$$\mathbf{A} = \begin{bmatrix} 0 & \sin^2(\theta_1) & \cos^2(\theta_1) & 0 & 2\cos(\theta_1)\sin(\theta_1) & 0 \\ \vdots & \vdots & \vdots & \vdots & \vdots & \vdots \\ 0 & \sin^2(\theta_{64}) & \cos^2(\theta_{64}) & 0 & 2\cos(\theta_{64})\sin(\theta_{64}) & 0 \\ \sin^2(\theta_1) & 0 & \cos^2(\theta_1) & 0 & 0 & -2\cos(\theta_1)\sin(\theta_1) \\ \vdots & \vdots & \vdots & \vdots & \vdots & \vdots \\ \sin^2(\theta_{64}) & 0 & \cos^2(\theta_{64}) & 0 & 0 & -2\cos(\theta_{64})\sin(\theta_{64}) \\ \cos^2(\theta_1) & \sin^2(\theta_1) & 0 & 2\cos(\theta_1)\sin(\theta_1) & 0 & 0 \\ \vdots & \vdots & \vdots & \vdots & \vdots & \vdots \\ \cos^2(\theta_{64}) & \sin^2(\theta_{64}) & 0 & 2\cos(\theta_{64})\sin(\theta_{64}) & 0 & 0 \end{bmatrix}$$

where the first 64 rows refer to rotations about the $+x_1$ axis, the middle 64 rows refer to rotations about the $+x_2$ axis and the final 64 rows refer to rotations about the $+x_3$ axis.

[6] In practice, there are several additional considerations involved in assembling the array of 192 directional susceptibility values to be used in conjunction with the design matrix in estimating the elements of $\bar{\mathbf{s}}$. First, the directional susceptibility values are subject to a phase lag (typically $\sim 20°$) imparted by the finite response time of the electronics. This phase angle is determined by measurement of an axial standard and applied to all subsequent data. Second, the directional susceptibility values measured during a rotation are deviatoric values, measured after zeroing out the bulk susceptibility to allow measurement of anisotropy at the most sensitive range. This necessitates a scaling that is accomplished with a single bulk measurement after the final spin. Third, rather than a single revolution, between 5 and 8 revolutions are acquired in each spin position depending on the magnitude of the anisotropy signal. The 192 directional susceptibility values used to determine the susceptibility tensor are averages from these multiple revolutions. Finally, the bridge circuit is susceptible to significant drift when measurements are made on the most sensitive range, as is commonly the case for weakly anisotropic samples.

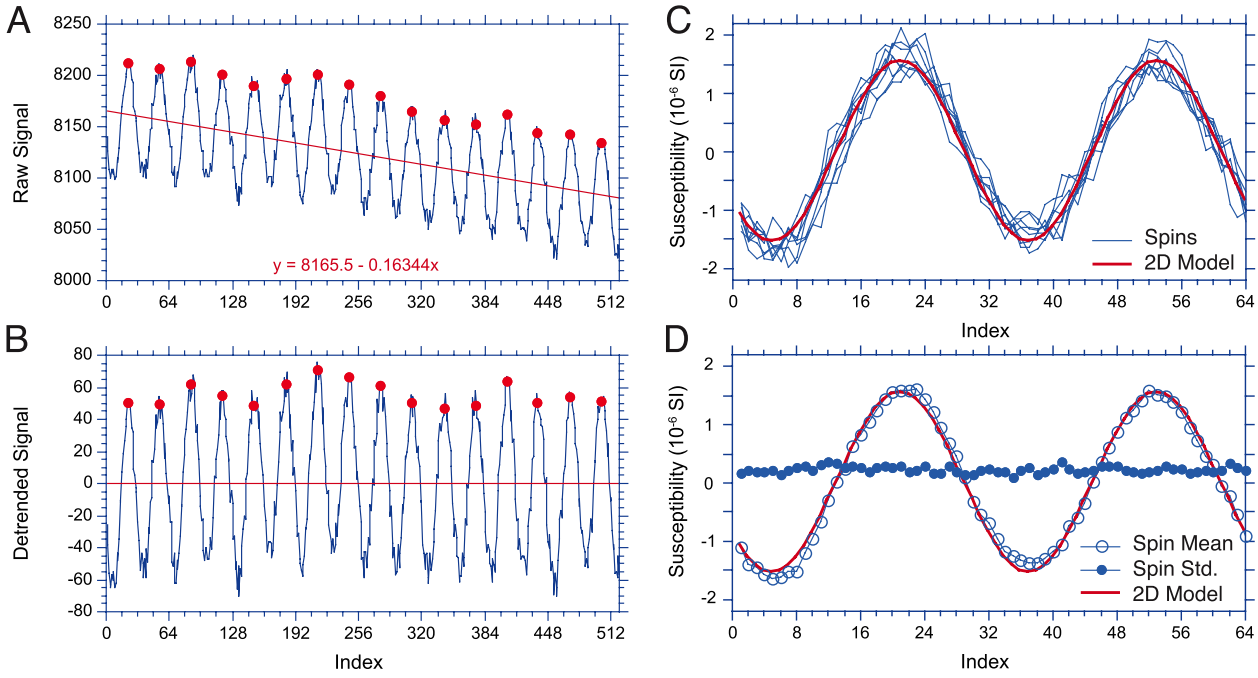

Figure 2. Processing steps for data from a single spin with eight revolutions. (a) Raw data with peaks (red dots) identified by peak-finding algorithm and best fit linear trend. (b) Detrended data. The linear trend in Figure 2a is removed only if this results in a smaller slope for the peaks. The mean value is removed regardless of whether linear detrending is applied. (c) Data from individual revolutions and best fit 2-D model. (d) Mean values (and standard deviations) from *n* revolutions compared to the best fit 2-D model.

[7] In the following sections we describe the steps involved in processing a single spin, the acquisition of bulk susceptibility data and how data from three spins and the bulk measurement are combined to yield the final susceptibility tensor. We highlight where this processing differs from that in the SUFAR program; the reader is referred to the documentation provided with the Kappabridge KLY-4S for a more complete description of the processing in the SUFAR program. We also examine the character of the instrument noise and document the suitability of the data for analysis using the linear perturbation techniques of *Hext* [1963].

3. Program AMSSpin

[8] Data from two files generated by the SUFAR program (CALKLY4.SAV and SUFAR.SAV) are read in during initial startup. The former file contains potentiometer settings and gain information for the range of applied fields (2–400 A/m) available for the KLY-4S. The latter file contains accepted values for the anisotropy standard supplied with the instrument, as well as gain values for the default applied field (300 A/m), phase lag, specimen holder and specimen volume information. Although some of this information (e.g., the anisotropy values for the specimen holder) are not used in the AMSSpin program, the structure of these files is maintained for compatibility with the SUFAR program.

3.1. Acquisition of Single Spin

[9] Susceptibility data are acquired at an angular sampling interval of 5.625° (64 samples/revolution) for multiple revolutions about each of three sample coordinate axes. The meter is zeroed with the specimen in the measurement region and so only deviatoric susceptibility variations are obtained. The autoranging function (enforced during startup) ensures that the susceptibility anisotropy is measured on the most sensitive range possible. Depending on the magnitude of anisotropy, five to eight complete revolutions (for the least sensitive to most sensitive ranges, respectively) plus an additional one eighth of a revolution are measured.

[10] The raw data from these multiple revolutions are contaminated by both instrumental noise and drift (Figure 2a). For many geological materials,

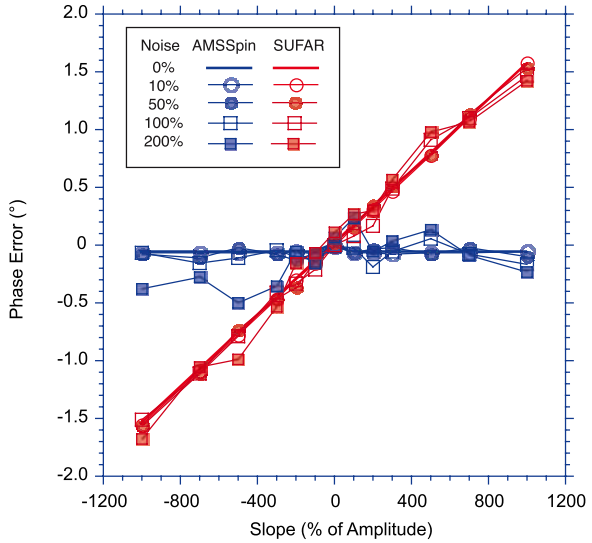

Figure 3. Comparison of phase information recovered for synthetic data using the method in the AMSSpin and SUFAR programs. Each point represents the average of 1000 synthetic data sets generated from a periodic signal plus noise and drift. Analysis of subsets of the data (half revolution + 8 points) used in the SUFAR program results in a slight bias toward higher phase values when the drift is toward more positive values (+slope) and toward lower phase values when the drift is toward more negative values.

the magnitude of the susceptibility anisotropy may be comparable to the drift (as much as a few 10^{-6} SI) and in such cases the drift will slightly affect the estimate of the phase of the susceptibility signal (see below). We remove a linear trend, approximating the drift, from the raw data if the detrended data yields a smaller overall slope for the peaks identified by a peak-finding algorithm (Figure 2b). The mean is then removed from the data (which are assumed to be deviatoric values with zero mean) and the values are scaled by the appropriate range correction factor ($10^{\text{range-5}}/3500$) and the anisotropy gain for the applied field ($\sim$1 for 300 A/m; note that two very similar gain settings, one for anisotropy and one for bulk measurements, are used following the convention of the SUFAR program). The amplitude and phase of the first harmonic (frequency 0.03125 sample^{-1}, corresponding to a half revolution of 32 points) are determined from the data (trimmed to an even number of revolutions) and are used to construct the best fit 2-D model for the data. Both the best fit 2-D model and the data are adjusted for the phase lag and the data from each spin are then subdivided into the component revolutions for display (Figure 2c). In order to facilitate display and (optional) output of the individual spin or revolution data, the data are resampled by spline interpolation (linear interpolation or phase shifting in the frequency domain yield comparable results) at 64 constant angular values beginning at 0°. The average values from n revolutions at each of these 64 positions are used for further processing and these average values as well as residuals relative to the 2-D model are displayed at the conclusion of a spin (Figure 2d).

[11] Our processing scheme for data from a single spin differs from that in the SUFAR program. In the SUFAR program, the sine and cosine components (or equivalently amplitude and phase) are determined separately for each half revolution (subsets of 40 points or 5/8 revolution are used) under the assumption that drift is negligible during the time ($\sim$1.25 s) needed for a half revolution. This assumption is generally reasonable, except in the case of very weakly anisotropic specimens (or specimen holder). We compared our processing method with that in the SUFAR program for a known periodic signal contaminated by a range of drift and noise values, using 1000 synthetic records in each test case (Figure 3). While both methods accurately recover the amplitude (within $\sim$0.1%), the method adopted in the SUFAR program results in a slight bias in the phase when drift over the full sequence of revolutions exceeds the specimen anisotropy.

3.2. Combining Spin Data to Tensor

[12] Once data from all three spins (with the specimen mounted in the positions shown in Figure 1) have been acquired, these data may be combined to calculate the deviatoric susceptibility tensor. The phase lag corrected data from spin one provide estimates of k_{33} and k_{22} (elements 1 and 17 of the 2-D model data array). Spin two yields estimates of k_{33} and k_{11} and spin three gives estimates for k_{11} and k_{22} (Figure 4a). Because the data from each spin are deviatoric susceptibilities, the estimates of a given tensor element from different spins will in general not be the same. This problem is analogous to the analysis of crossover errors in marine geophysical data. We therefore adopt the method of *Prince and Forsyth* [1984] to find the offsets (z_1, z_2, z_3 for spins 1, 2, 3) that will minimize the misfits between the two estimates of the same tensor element. For crossover errors (**b**) defined by

$$\mathbf{b} = \begin{bmatrix} k_{33}(Spin1) - k_{33}(Spin2) \\ k_{11}(Spin2) - k_{11}(Spin3) \\ k_{22}(Spin3) - k_{22}(Spin1) \end{bmatrix}$$

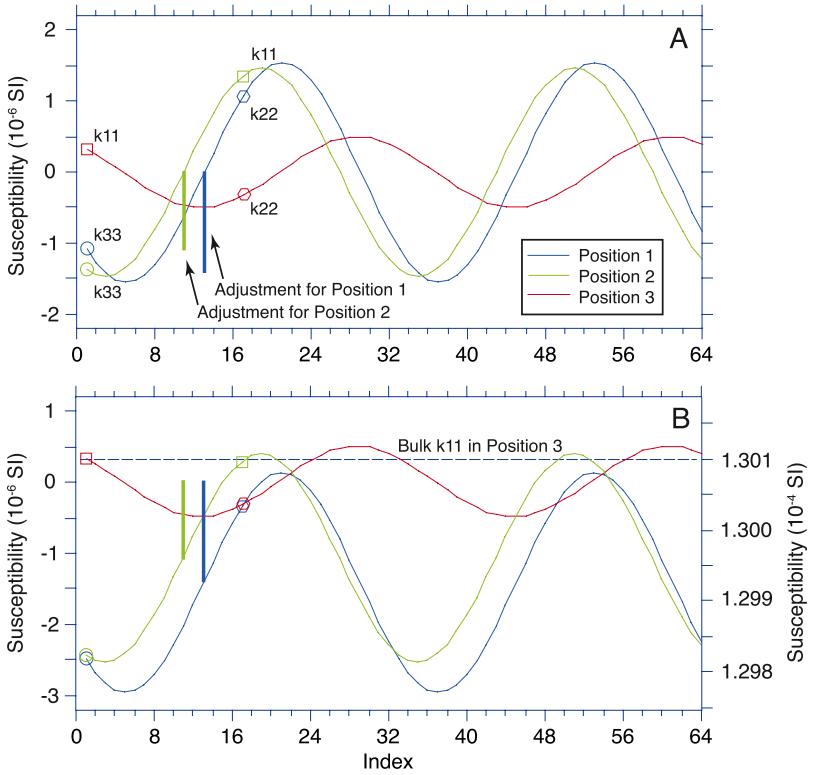

Figure 4. Crossover adjustment for data from three spins. (a) Original (zero-mean) deviatoric susceptibility data from three spins. The best fit 2-D model for each spin provides an estimate of two elements of the deviatoric susceptibility tensor (square, k_{11}; hexagon, k_{22}; circle, k_{33}). Thick bars indicate the calculated offsets for spins 1 and 2. (b) Crossover-adjusted data illustrating the better agreement of estimates of tensor elements. The deviatoric susceptibility data are scaled to absolute values (right-hand scale) using a bulk measurement in spin position 3, corresponding to k_{11}.

the best fit offsets (**z**) in a least squares sense are given by the solution to **Cz** = **b** where

$$\mathbf{C} = \begin{bmatrix} -1 & 1 & 0 \\ 0 & -1 & 0 \\ 1 & 0 & 0 \end{bmatrix}$$

and column 3 (corresponding to spin 3) has been set to zero such that offsets are relative to the data from spin 3. Adding these offsets to the 2-D models for each spin typically results in a crossover error on the order of a few 10^{-8} SI (this value is recorded in the output record). These offsets are added to the 64 mean values for each spin. The resulting 192 crossover adjusted mean values, following the scaling by a bulk measurement described below, are then used to calculate the final susceptibility tensor.

[13] A single bulk susceptibility measurement is used to scale the crossover-adjusted deviatoric susceptibility values to absolute susceptibility values. Acquisition of a bulk susceptibility estimate on the KLY-4S involves an initial baseline (100 measurements), sample (200 measurements), and a final baseline (100 measurements) (Figure 5). The processing of these data differs for range 1 and the remaining, less sensitive ranges. For specimens with susceptibilities sufficiently low to be measured on range 1, both baselines and the bulk measurement all occur on the same range. In this case, a linear regression of data from the two baselines is used to remove both the baseline value as well as the instrumental drift from the raw data for the specimen. The second baseline measurement is always made on the same range as for the sample. For specimens measured on ranges 2, 3 or 4, only data from the second baseline may be used to correct the specimen measurement data (the mean baseline value is subtracted from the raw data for the specimen) and no drift correction is made. Regardless of range, the resulting raw value is scaled by the appropriate range correction factor ($10^{\text{range-5}}/3500$) and the bulk gain value for the applied field (also $\sim$1 for 300 A/m) to yield the final susceptibility in SI units.

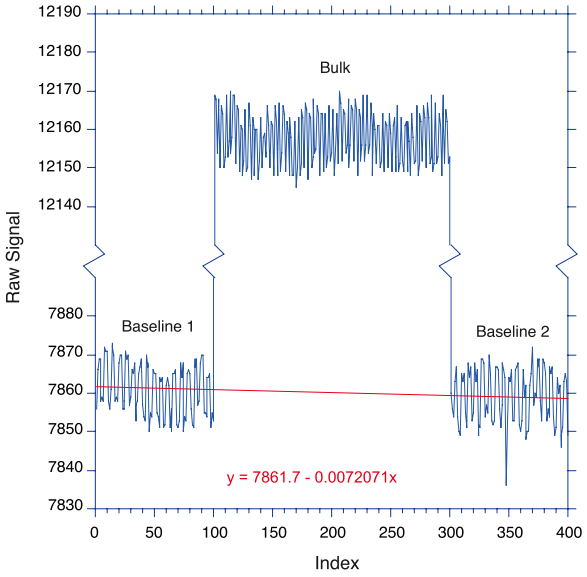

Figure 5. Example of raw data used to derive bulk susceptibility measurement on range 1. Linear trends of data from initial and final baselines are used to remove baseline and drift from the intervening specimen bulk susceptibility.

[14] The single bulk measurement used to scale the deviatoric susceptibility values is measured immediately following spin 3, with the specimen at an angle of $\theta = 0$ corresponding to k_{11}. All 192 mean deviatoric susceptibility values (**D**) are adjusted accordingly and are used in conjunction with equation (2) and the design matrix to calculate the six independent elements of the best fit susceptibility tensor, $\bar{\mathbf{s}}$. The bulk susceptibility is recalculated from the average of the trace of the best fit susceptibility tensor. It should be noted that various combinations of incorrect specimen orientations will also yield internally consistent (though incorrect) tensors. Such orientation errors could be more readily detected by measuring a bulk susceptibility following each spin, however, we have opted to rely on the care of the operator and use a single bulk measurement as in the original SUFAR program.

[15] After completion of the three spins and bulk measurement, the mean data for each position are displayed together with the best fit 3-D model (Figures 6a–6c), calculated from $\bar{\mathbf{s}}$ using equation (1). The predicted values for the three spins may then be used to calculate (and optionally display) residuals. These residuals form the basis for various statistical tests of anisotropy (see below) and patterned residuals may provide an indication of improper specimen centering, inhomogeneity or other instrumental problems (Figures 6d–6f). The residuals as well as the mean data and best fit 3-D model are displayed after normalization by the trace of the final best fit tensor.

[16] Our technique for calculating the best fit tensor differs considerably from that used in the SUFAR program. In the SUFAR program, the independent tensor elements of the deviatoric tensor are obtained from estimates of the sine and cosine components in the three measurement positions [*Jelinek*, 1995]. To provide simultaneous estimates of measurement errors, the data from each measurement position are divided into two partial measurements (the average sine and cosine components for the first and last half of a spin). As noted in the manual accompanying the instrument, the associated statistical analysis and tests for anisotropy are "rather complex" [*Jelinek*, 1995]. In contrast, our method of constructing the best fit tensor utilizes 192 susceptibility values (each an average from multiple revolutions) and a methodology analogous to that developed for the smaller number of measurements used in previous static measurement systems. A significant benefit of this approach is that the linear perturbation analysis techniques [*Hext*, 1963; *Jelinek*, 1977, 1978] applied to previous data sets are readily extended to the more numerous data acquired by the Kappabridge KLY-4S.

4. Statistical Analysis

[17] The application of linear perturbation analysis to AMS data [*Hext*, 1963] is based on the assumption that each directional susceptibility measurement includes an unknown measurement error and that these errors are small (relative to the directional susceptibility), normally distributed with zero mean, and uncorrelated. To the extent that these conditions are met, the estimated variance

$$\sigma^2 = \frac{\sum_i \delta_i^2}{n_f}$$

(where n_f is the number of degrees of freedom, here 192–6 or 186, and δ_i is the measurement error as defined in equation (3)) may be used to estimate the angular uncertainties of the eigenvectors of the susceptibility tensor as well as to provide statistical tests of anisotropy based on the eigenvalues [see *Hext*, 1963; *Jelinek*, 1977, 1978; *Tauxe*, 1998].

[18] In order to evaluate whether the assumptions above are valid, it is useful to examine the instru-

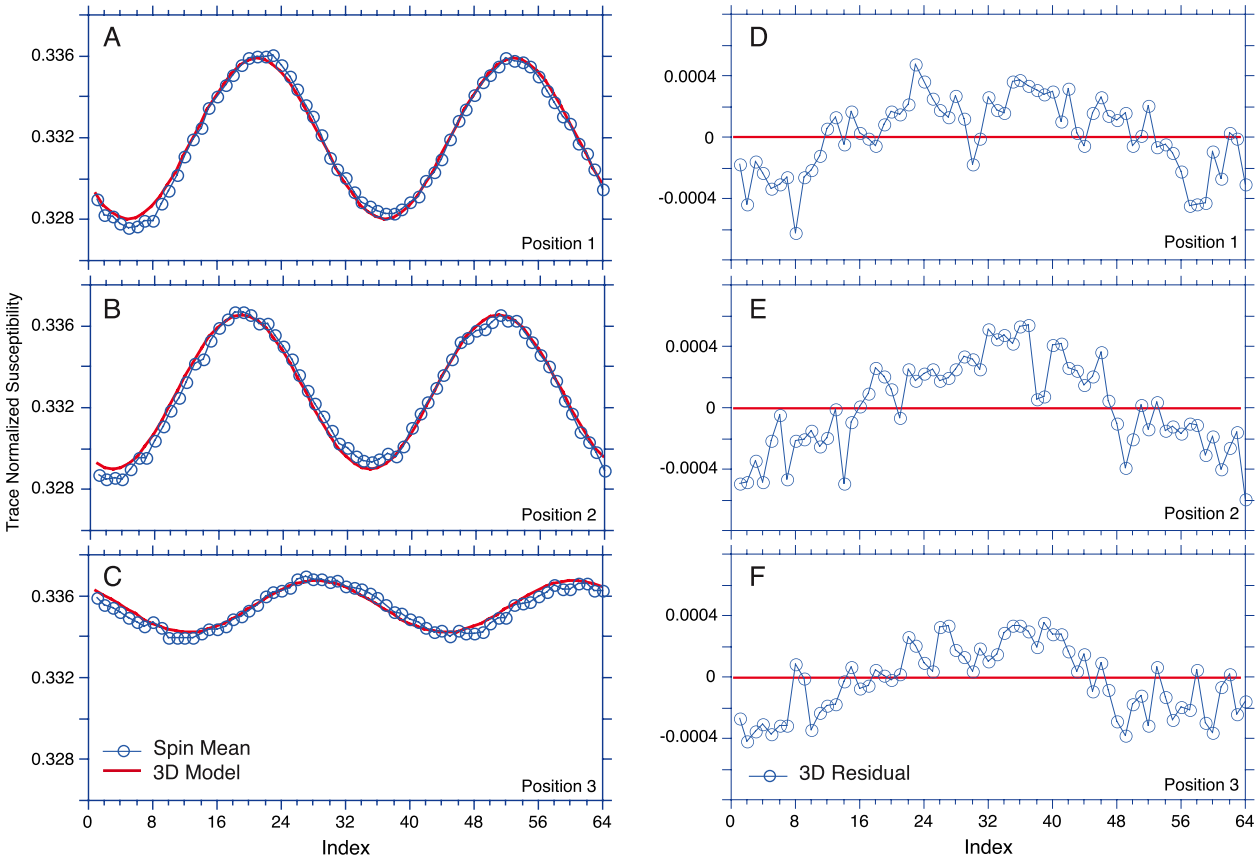

Figure 6. Comparison of final scaled susceptibility data and 3-D model. (a–c) Mean susceptibility values for each spin and the corresponding best fit 3-D models from the susceptibility tensor. (d–f) Residuals (observed – model). All values have been normalized by the trace of the susceptibility tensor.

mental noise and drift. Multiple measurements of the empty specimen holder illustrate several relevant features of the instrumental noise and drift (Figure 7). These data indicate a typical instrumental noise level of $\sim$3 to 5 $\times$ 10^{-7} SI, with a distinct peak at about 0.2 sample^{-1} (corresponding to $\sim$12 cycles/revolution). The origin of this noise is unknown. Measurements of the empty specimen holder also illustrate that both the magnitude and sense of drift can vary significantly and that the drift is not perfectly linear. We find that the noise and drift characteristics make it difficult to accurately determine the anisotropy of the specimen holder (this anisotropic signal is subtracted in the SUFAR program). This is perhaps best illustrated by the average power spectra (Figure 7b), where there is little if any indication of significant power at the frequency (0.03125 sample^{-1}) corresponding to a half revolution. We therefore treat the specimen holder as isotropic, subtracting its scalar magnitude from the bulk measurement of spin position 3 prior to scaling the data from all three spins to absolute susceptibility values.

[19] The 192 measurement directional susceptibility data that we use to derive the best fit susceptibility tensor each represent the average of multiple measurements obtained during n specimen revolutions. Given that instrumental drift is not perfectly linear, it is reasonable to ask how our processing scheme (which begins by removal of a linear trend approximating this drift) affects the measurement errors. Figure 8 compares the distribution of residuals for the 192 mean directional susceptibilities with the residuals for the original 1536 measurements used to calculate the mean values. Both sets of residuals are statistically indistinguishable from a normal distribution (based on a Kolmogorov-Smirnov test; see Figure 8 caption). Moreover, the standard deviation of the residuals from the 192 mean values is a factor of 2.6 lower than that of the standard deviation for the full set of original values. This reduction is close to the factor of 2.8 reduction ($1/\sqrt{n}$) expected from averaging data from 8 revolutions, suggesting that deviations from linear drift do not introduce a large bias into the average values used to calculate the

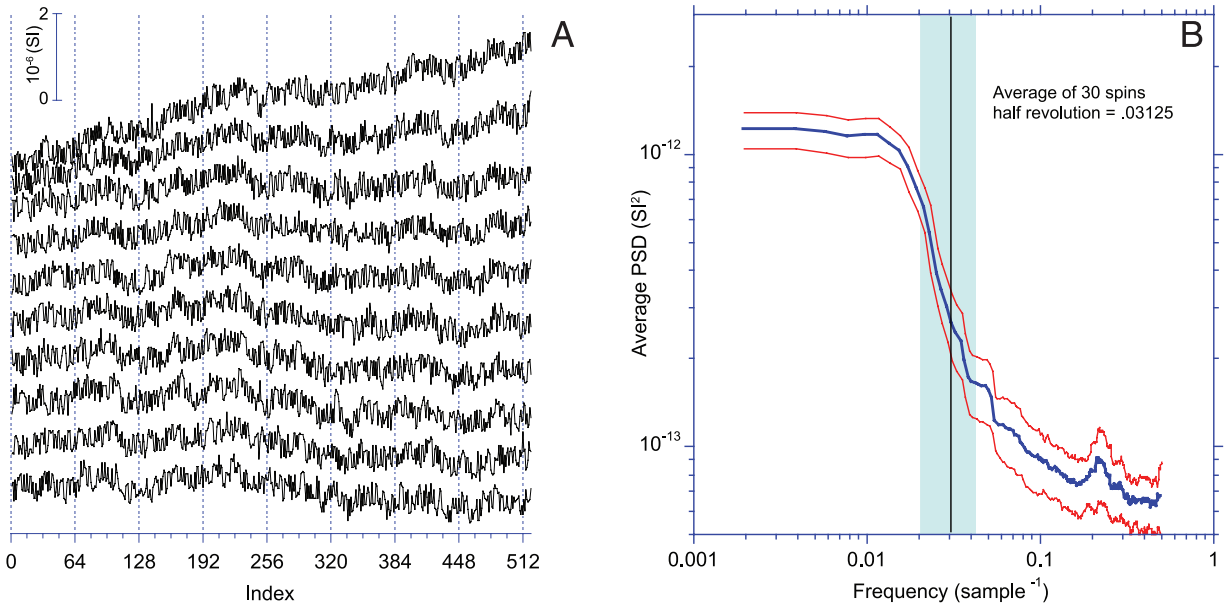

Figure 7. Instrumental drift and noise for the Kappabridge KLY-4S. (a) Representative data from spins (8 revolutions; boundaries denoted by dotted vertical lines) of empty specimen holder (i.e., ring with 64 notches only, without cube). (b) Average multitaper power spectral density (1 σ errors in red) based on detrended data from 30 spins with empty specimen holder, including the data shown in Figure 7a. Note the lack of a distinct peak at 0.03125 sample^{-1}, corresponding to a half revolution. The frequency resolution of the multitaper estimate is shown by the blue vertical band.

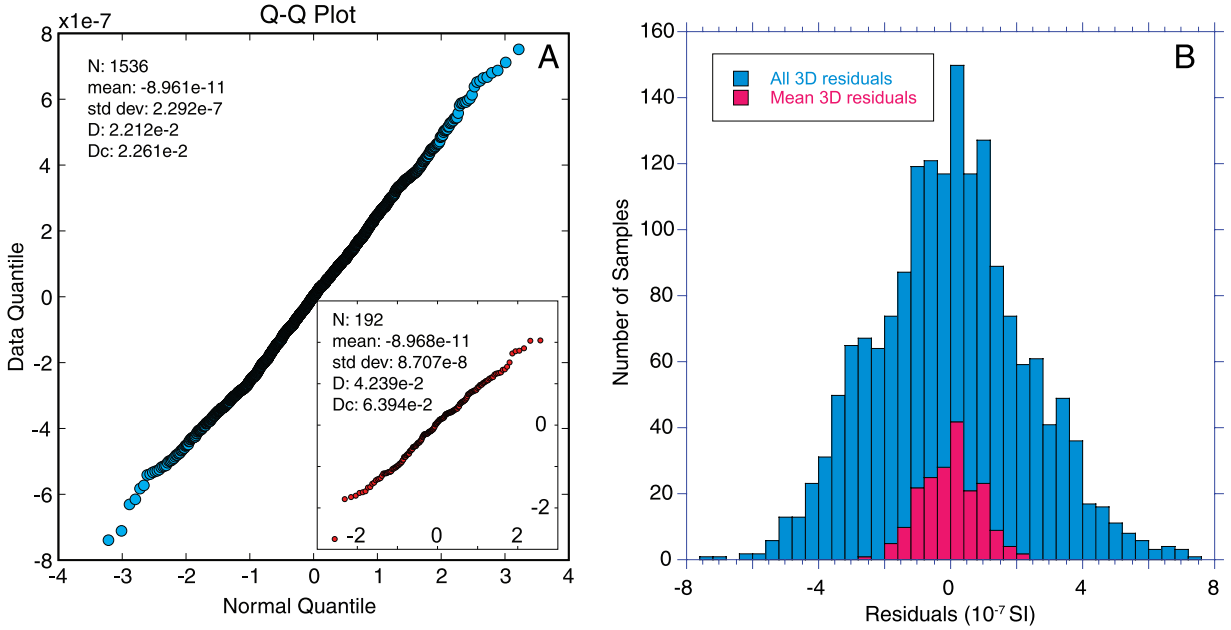

Figure 8. Distribution of residuals for a representative specimen. (a) Quantile-quantile plot for all data acquired and for the 192 averaged values (inset). Both distributions are statistically indistinguishable from a normal distribution based on Kolmogorov-Smirnov (K-S) test (D, K-S statistic; Dc, critical value). (b) Histograms of residuals for all data acquired (blue) and for the 192 averaged values (red) used in calculating the final susceptibility tensor.

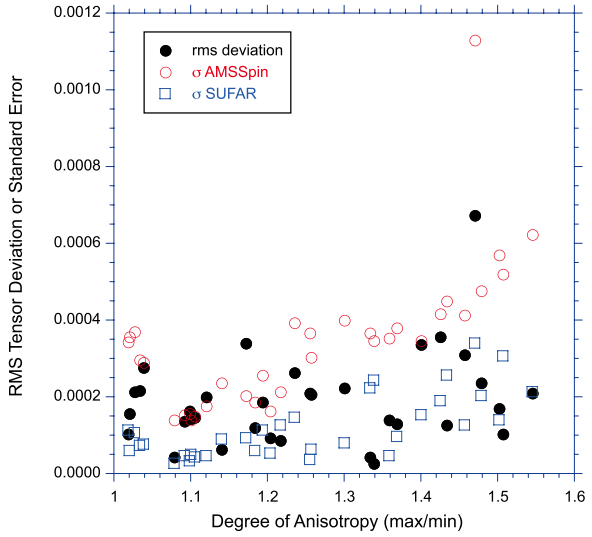

Figure 9. Comparison of susceptibility tensors derived by processing the same raw data using the AMSSpin program and algorithm in SUFAR program.

susceptibility tensor. The RMS magnitude of the 192 mean residuals is small (8×10^{-8} SI relative to the bulk susceptibility of 1.3×10^{-4} SI for the specimen in Figure 8) and these residuals are normally distributed with zero mean. While the residuals may not be independent in all cases (particularly when the sample is poorly centered or inhomogeneous), it appears that the assumptions of the linear perturbation analysis are generally satisfied.

[20] The formulations developed for estimating the uncertainties on the eigenvectors of the susceptibility tensor and the statistical tests for anisotropy [*Hext*, 1963] can be applied with minor modifications for the number of degrees of freedom. Specifically, the semi-angles of the confidence ellipses for the eigenvectors are given by

$$\varepsilon_{21} = \varepsilon_{12} = \tan^{-1}\left[f\sigma/2(\tau_1 - \tau_2)\right]$$

$$\varepsilon_{32} = \varepsilon_{23} = \tan^{-1}\left[f\sigma/2(\tau_2 - \tau_3)\right]$$

$$\varepsilon_{31} = \varepsilon_{13} = \tan^{-1}\left[f\sigma/2(\tau_1 - \tau_3)\right]$$

where $\tau_1 \geq \tau_2 \geq \tau_3$ are the eigenvalues and

$$f = \sqrt{2\left(F_{(2,n_f)}; (1-p)\right)} = \sqrt{2\left(F_{(2,186)}; (1-0.05)\right)}$$
$$= \sqrt{2(3.04)} = 2.465$$

for $n_f = 192 - 6$ or 186 degrees of freedom at the 95% confidence level. The corresponding F tests for anisotropy remain the same as for susceptibility tensors based on a smaller number of measurement positions:

$$F = 0.4\left(\tau_1^2 + \tau_2^2 + \tau_3^2 - 3\chi_b^2\right)/\sigma^2$$
$$F_{12} = 0.5[(\tau_1 - \tau_2)/\sigma]^2$$
$$F_{23} = 0.5[(\tau_2 - \tau_3)/\sigma]^2$$

where the bulk susceptibility (χ_b) is given by $\chi_b = (\bar{s}_1 + \bar{s}_2 + \bar{s}_3)/3$. The critical values (at the 95% confidence level) for the F tests also remain the same. The susceptibility tensor is statistically isotropic if $F < 3.4817$ and is statistically oblate if $F_{12} < 4.2565$ or statistically prolate if $F_{23} < 4.2565$.

[21] It should be noted that uncertainty estimates for the eigenvectors that are displayed at the completion of a measurement in the AMSSpin program differ from those in the SUFAR program. The former are based on linear perturbation analysis [*Hext*, 1963; *Jelinek*, 1977, 1978] in which error angles are defined along the principal planes of the susceptibility ellipsoid whereas in the SUFAR program these error angles are oblique, reflecting the interplay between the orientations of principal planes and measuring planes. Nevertheless, the numerical values provided by the these approaches are similar, characterizing the uncertainties in determination of the principal directions in a very similar way.

5. Comparison of Results With SUFAR Program

[22] The treatment of directional susceptibility data in the AMSSpin program differs from that in the SUFAR program and so it is not surprising that the calculated tensors differ somewhat. In order to compare the results from our new program and the SUFAR program, we first measured a suite of 33 specimens with a range of anisotropy values (ratio of max/min eigenvalues = 1.02–1.55) with both programs. Bulk susceptibilities from the two programs agree well (mean difference = 0.3%). The root mean square (rms) deviation of the six independent elements (normalized by the trace) of the susceptibility tensors from these two measurements differ by an average of 0.0009. Although this discrepancy is large relative to the standard error, differences in the two measurements also include uncertainties in positioning the specimen in the specimen holder.

[23] A more direct test is to compare the tensors obtained by processing the same raw data by both

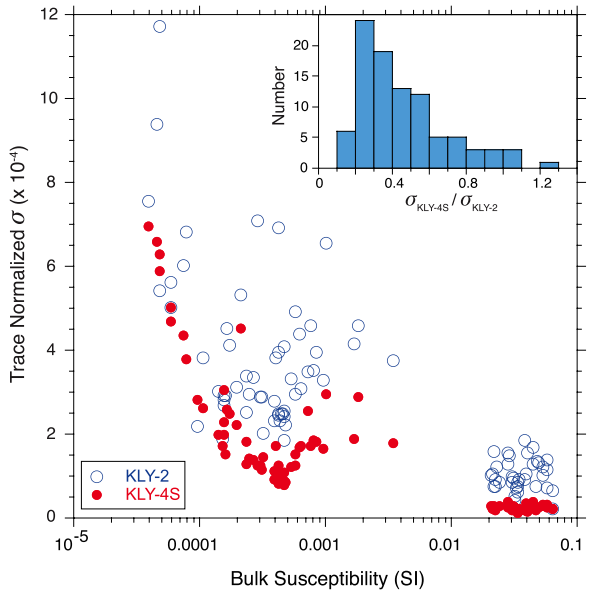

Figure A1. Comparison of measurement errors (as quantified by the trace normalized value of sigma) for the Kappabridge KLY-4S and KLY-2. Inset shows a histogram of the ratio of uncertainties (KLY-4S/KLY-2).

the method developed for the AMSSpin program and the processing algorithm of the SUFAR program. The RMS deviations of the susceptibility tensors derived by these two processing techniques averages ~0.0002, with slightly larger RMS deviations for specimens with higher degrees of anisotropy (Figure 9). For all but two of these 33 specimens the RMS deviation is less than the standard error (σ) calculated from the AMSSpin program (this error estimate is on average 3.5 times that of the SUFAR program). Comparison of multiple measurements of these same samples (measured on different days) using the AMSSpin program suggests that specimen orientation errors are comparable to the standard error (rms deviations average 0.0003). On the basis of these comparisons, we suggest that differences between the processing methods in the AMSSpin and SUFAR programs are smaller than or comparable to uncertainties associated with specimen positioning.

6. Conclusions

[24] We have developed a graphical program that allows the acquisition of AMS data from the Kappabridge KLY-4S. This program provides real time display of susceptibility data acquired during a spin and the display of best fit 2-D and 3-D models to the data (and the resulting residuals). In addition, the program allows the display of all previously measured data from a specimen (sample, site, or study) together with the current specimen results to allow evaluation of within site consistency. The treatment of the sample holder as isotropic, processing of the data from an individual spin, as well as the method of combining the three spins to yield the final susceptibility tensor, differ significantly from the methods used in the SUFAR program. Despite the different processing methods the AMSSpin and SUFAR programs yield results that are quite similar, with deviations that are comparable to or smaller than uncertainties introduced by sample positioning. We find that by utilizing mean directional susceptibility values for 192 positions that the measurement errors are suitable for linear perturbation analysis, providing a well established means of statistically characterizing the AMS data acquired with the Kappabridge KLY-4S.

[25] An executable version of the LabVIEW program, together with additional documentation, is available from the EarthRef.org Digital Archive (ERDA) at http://earthref.org. Although the program is presently available only for a Macintosh, the source code is platform independent and will be ported to other platforms in the future. Modifications that will allow use of the program with a KLY-3S are also underway. Output from this program can be converted to the MAGIC standard format for plotting with the PmagPy software that is also available at this same site (see Appendix A for example output).

Appendix A

[26] To validate the new AMSSpin program, we have also compared the results from this program (and the Kappabridge KLY-4S) with results obtained from a Kappabridge KLY-2 static measurement system. AMS measurements were made on both instruments for approximately 100 samples, with bulk susceptibilities ranging from 4×10^{-5} to 7×10^{-2} SI. Bulk susceptibilities with the two instruments typically agree within 0.5%, with maximum deviations of approximately 3%. The Kappabridge KLY-4S and AMSSpin program yield better defined susceptibility tensors (as measured by the standard error, sigma). On average sigma values are a factor of 2–3 smaller than those determined with the Kappabridge KLY-2, as expected from the larger number of measurements using the KLY-4S, though the improvement is less pronounced in samples with lower bulk susceptibilities (Figure A1). The value of sigma also varies

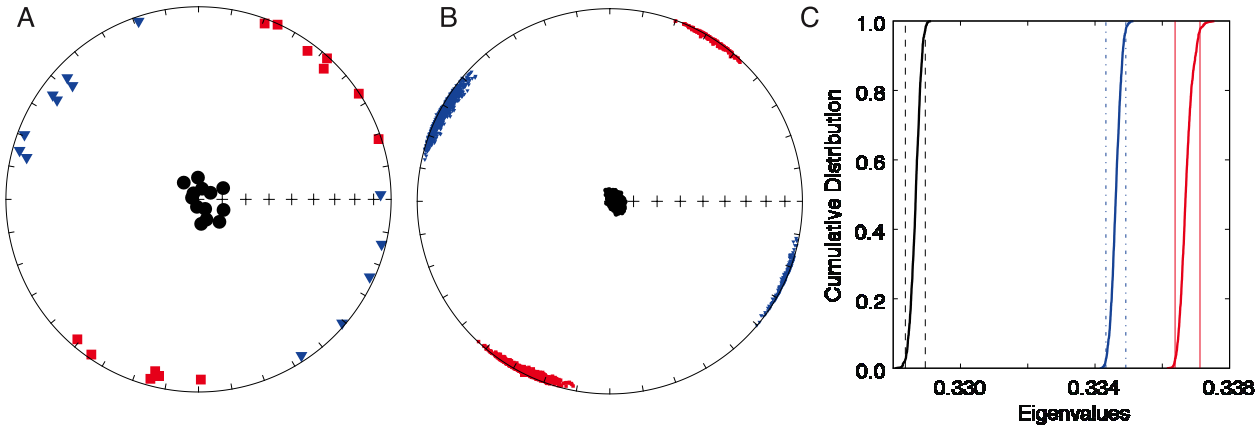

Figure A2. Example output from processing software of the PmagPy software distribution. (a) Equal area plot of eigenvectors for specimens from a single sampling site. Circles, triangles, and squares represent the eigenvectors associated with the minimum, intermediate, and maximum eigenvalues, respectively. (b) Nonparametric bootstrap pseudosamples generated from the specimen data shown in Figure A2a. (c) Cumulative distribution functions for the eigenvalues of bootstrap pseudosamples. Vertical lines indicate the 95% confidence bounds of the site mean eigenvalues.

both as a function of applied field and measurement range, with higher values at lower applied fields and when susceptibilities are at the lower end of a measurement range. Differences in the susceptibility tensors from the two instruments are also a function of bulk susceptibility. For specimens with susceptibilities of $\sim 10^{-4}$ SI, the root mean square difference in the six independent susceptibility tensor elements (normalized by the trace) is approximately 0.001 and this deviation decreases to about 0.0001 for a bulk susceptibility of $\sim 10^{-1}$ SI.

[27] The standard output of the AMSSpin program includes a minimal amount of information: the specimen name, the six independent elements of the susceptibility tensor (trace normalized, in specimen coordinates) and sigma, the bulk susceptibility and a small number of parameters (e.g., volume, applied field) relevant to the measurement. Software available with the PmagPy distribution allows conversion of the data from AMSSpin to the standard MAGIC format. Data can be analyzed in a variety of ways (e.g., generating error ellipses for a site using either bootstrap resampling or Hext statistics) and plotted in a variety of coordinate systems (see Figure A2 for sample output).

[28] While the errors associated with measurements on the Kappabridge KLY-4S are typically small and normally distributed for most specimens, we have found that this is not the case for some samples. Figure A3 illustrates results from a basaltic dike with a high bulk susceptibility (6.3×10^{-2} SI) and a very low degree of anisotropy. In

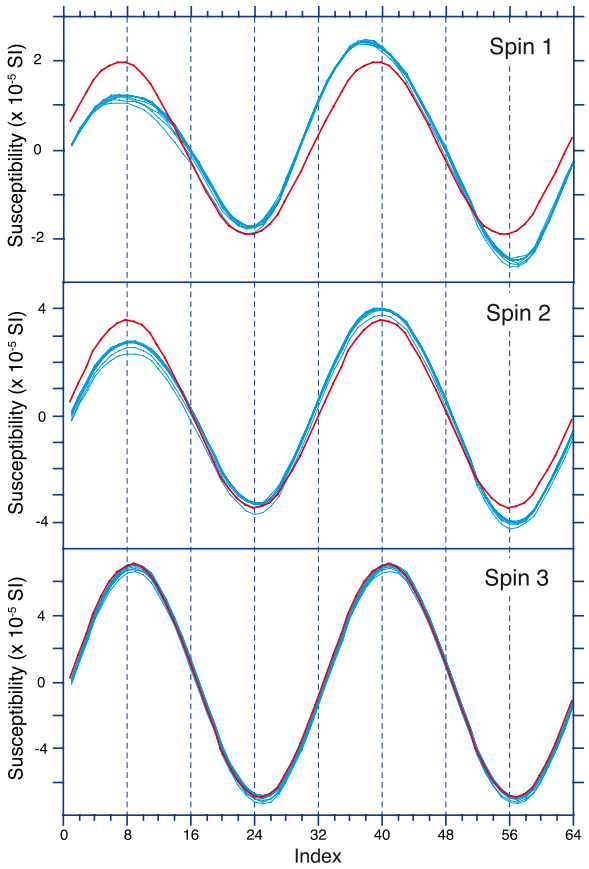

Figure A3. Example of specimen with directional susceptibility variations deviating significantly from that expected from a symmetric second-order tensor. Deviatoric susceptibility data for each revolution are shown in blue and the best fit 2-D model is shown in red for each of the three spins. Note that each plot has a different vertical scale.

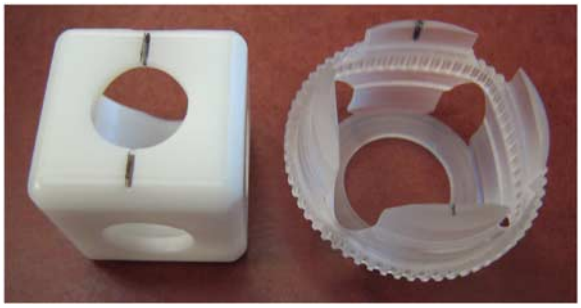

Figure A4. Cubic specimen holder and cog used for positioning standard 2.54 cm diameter cores.

this case, the directional susceptibility signal for spins 1 and 2 deviates substantially from that expected from a symmetric second-order tensor. Such deviations may arise from inhomogeneity within the specimen (or possibly from other artifacts of the measurement system such as the specimen being offset from the center of the coil). By displaying the measured and best fit 2-D and 3-D models to the data, the AMSSpin program provides the user with a means of identifying such data as problematic.

[29] The confidence intervals for the principal susceptibility values are affected by the orientation of the measurements relative to the anisotropic susceptibility of the specimen [*Hext*, 1963; *Owens*, 2000]. This effect can be minimized by the use of a measurement scheme that is rotatable [*Hext*, 1963], i.e., one in which the measurements are evenly spaced over the unit sphere such that error variances do not depend on the relative orientation of the specimen and measurement positions. The directional susceptibility data acquired at evenly spaced intervals during each spin constitute such a rotatable design for determining the susceptibility tensor in each plane. The distribution of measurement positions on three orthogonal planes, however, inevitably introduces a small degree of nonrotatability in the measurement design. Although the processing differs in the AMSSpin program and the SUFAR program, both approaches utilize the same directional measurements and therefore are affected by this nonrotatability. We note that the addition of spins about two diagonal rotation axes in the specimen coordinate system could be introduced to further improve the rotatability.

[30] Finally, we have found that a cubic specimen holder (in which standard 2.54 cm diameter cores can be placed) facilitates the measurement of AMS on the Kappabridge KLY-4S. This holder provides an internally consistent specimen position in the three spin positions and simplifies the placement of the specimen in the required three orthogonal planes. The cubic specimen holder accommodates cores up to $\sim$2.4 cm in length and this cube is placed in a modified cog (Figure A4) that replaces the holder provided with the instrument. The combined cog and cube specimen holder system has a bulk susceptibility (-8×10^{-6} SI) only slightly higher than for the original specimen holder. Inquiries about the modified specimen holder should be directed to the first author.

Acknowledgments

[31] We thank AGICO for providing the source code for the SUFAR program and for their kind assistance during development of the AMSSpin program. We also thank M. Jackson, F. Hrouda, J. Pokorny, and an anonymous reviewer for comments that improved the text. The development of the software was supported by NSF OCE0221948.

References

Hext, G. (1963), The estimation of second-order tensors, with related tests and designs, *Biometrika*, *50*, 353–357.

Jelinek, V. (1977), *The Statistical Theory of Measuring Anisotropy of Magnetic Susceptibility of Rocks and Its Application*, 88 pp., Geofyzika, Brno., Czech Republic.

Jelinek, V. (1978), Statistical processing of anisotropy of magnetic susceptibility measured on groups of specimens, *Stud. Geophys. Geod.*, *22*, 50–62, doi:10.1007/BF01613632.

Jelinek, V. (1995), Measuring anisotropy of magnetic susceptibility on a slowly spinning specimen—Basic theory, *AGICO Print 10*, 27 pp., Adv. Geosci. Instrum. Co., Brno, Czech Republic.

Jelinek, V., and J. Pokorny (1997), Some new concepts in technology of transformer bridges for measuring susceptibility anisotropy of rocks, *Phys. Chem. Earth*, *22*, 179–181, doi:10.1016/S0079-1946(97)00099-2.

Owens, W. H. (2000), Statistical applications to second-rank tensors in magnetic fabric analysis, *Geophys. J. Int.*, *142*, 527–538, doi:10.1046/j.1365-246x.2000.00174.x.

Pokorny, J., P. Suza, and F. Hrouda (2004), Anisotropy of magnetic susceptibility of rocks measured in variable weak magnetic fields using the KLY-4S Kappabridge, in *Magnetic Fabric: Methods and Applications*, edited by F. Martín-Hernández et al., *Geol. Soc. Spec. Publ.*, *238*, 69–76.

Prince, R. A., and D. W. Forsyth (1984), A simple objective method for minimizing cross-over errors in marine gravity data, *Geophysics*, *49*, 1070–1083, doi:10.1190/1.1441722.

Rochette, P., M. Jackson, and C. Aubourg (1992), Rock magnetism and the interpretation of anisotropy of magnetic susceptibility, *Rev. Geophys.*, *30*, 209–226, doi:10.1029/92RG00733.

Tarling, D. H., and F. Hrouda (1993), *The Magnetic Anisotropy of Rocks*, 217 pp., Chapman and Hall, London.

Tauxe, L. (1998), *Paleomagnetic Principles and Practice*, 299 pp., Kluwer Acad., Dordrecht, Netherlands.